Developing and verifying a quantitative dissolution model for metal-bearing nanoparticles in aqueous media

Song, Y.; Rottschäfer, V.; Vijver, M.G.; Peijnenburg, W.J.G.M.

Environmental Science Nano

ROYAL SOCIETY OF CHEMISTRY

PAPER

View Article Online
View Journal | View Issue

Cite this: *Environ. Sci.: Nano*, 2023, **10**, 1790

Developing and verifying a quantitative dissolution model for metal-bearing nanoparticles in aqueous media†

Yuchao Song, *[a] Vivi Rottschäfer, [bc] Martina G. Vijver [a] and Willie J. G. M. Peijnenburg [ad]

Received 14th February 2023,
Accepted 26th May 2023

DOI: 10.1039/d3en00096f

rsc.li/es-nano

Dissolution of nanoparticles (NPs) determines the fate and subsequently the actual exposure of biota to the NPs. Whether and to what extent NPs dissolve or remain in their particulate form in aqueous media is thus of pivotal knowledge for the safety assessments of NPs. In this research, secondary data on dissolution of NPs were systematically collected. A range of dissolution rates could be recalculated, as dependent on the characteristics of the NPs and the exposure medium. For example, two nanoparticles which are identical in terms of chemical composition of the particle core and of the coating, had a fully different dissolution behaviour, as subject to different surface modifications. A model was derived for calculating dissolution rate constants of NPs. The model is based on the initial kinetics of dissolution of NPs under different exposure scenarios and on the assumption of pseudo-first order reaction kinetics at the particle surface. Characterizing the dissolution rates and the parameters which modify dissolution allows for grouping of those NPs that dissolve either very slowly or very quickly. This information can be used for risk assessment of NPs, and once sufficient kinetic dissolution data are available, will ultimately allow for development of predictive models for the dissolution kinetics of newly developed nanomaterials.

Environmental significance

Nanoparticles are increasingly used in various consumer products, and their release into the environment through wastewater and other pathways is a growing concern. The ability to quantify the dissolution of these nanoparticles using pseudo-first order kinetics provides a valuable tool for assessing their potential environmental impact. The model developed for grouping NPs based on their dissolution kinetics has important implications for hazard assessment. By understanding the kinetics of dissolution for different types of nanoparticles, it is possible to predict their behavior in the environment and potential impacts on ecosystems and human health. This information can be used to guide decisions regarding the use and regulation of these materials, ultimately promoting more sustainable and responsible practices. Overall, the findings of this study highlight the importance of understanding the behavior of metallic nanoparticles in the environment and provide a valuable tool for assessing their potential impacts. The use of this method has the potential to inform policy decisions and promote more sustainable practices in the use and regulation of nanomaterials.

1. Introduction

Widespread usage of engineered metal-bearing nanoparticles (NPs) has enormously increased over the last few decades, and these particles will inevitably enter the environment and exert possible impacts on human and ecosystem health.[1,2] Numerous studies have been published to explore the toxicity of NPs to a variety of organisms such as microorganisms,[3] algae,[4] fungi,[5] plants,[6] and piscine and mammalian cells.[7,8]

Metal-based nanomaterials comprise a significant portion of the initial generation of nanomaterials. On the basis of especially the chemical composition and also the inherent nano-specific properties of the particles, a distinction can be made between non-soluble metal-bearing NPs and metal-bearing NPs that release metal ions from their surface once dispersed into an aqueous medium. The biological response to metal-based nanoparticle (NP) suspensions has been extensively documented and can be attributed to the

[a] *Institute of Environmental Sciences (CML), Leiden University, Einsteinweg 2, 2333 CC Leiden, The Netherlands. E-mail: y.song@cml.leidenuniv.nl*
[b] *Mathematical Institute, Leiden University, Niels Bohrweg 1, 2333 CA Leiden, The Netherlands*
[c] *Korteweg-de Vries Institute for Mathematics, University of Amsterdam, P.O. Box 94248, 1090 GE Amsterdam, The Netherlands*
[d] *Center for Safety of Substances and Products, National Institute of Public Health and the Environment (RIVM), P.O. Box 1, Bilthoven, The Netherlands*
† Electronic supplementary information (ESI) available. See DOI: https://doi.org/10.1039/d3en00096f

combined effects of the particulate characteristics of the NPs and the subsequent release of metal ions. This means that alteration of the dissolution kinetics will modify the toxic response[9–11] because the ratio of particles and ions in the suspension will change over time.

Numerous results of nanotoxicological studies have been reported in the last decade, however the challenge is the lack of standardization of tested protocols across published results up till now. This resulted in different test media being used with variable exposure conditions, while the dynamics of the actual exposure concentrations experienced by the selected test organisms are not always reported. These dynamics of exposure include especially chemical transformation and particle sedimentation in the exposure media.[12] The particle characteristics as well as the medium composition drive the dissolution and aggregation kinetics of particles.[13,14] It hence is important to quantify the dissolution of NPs in nanotoxicological studies in which dissolution is amongst others accompanied by particle aggregation and sedimentation.

Dissolution starts once particles enter the medium and is a dynamic process in which ions constantly migrate from the particle surface to the solution, until the ion concentration reaches a steady state level in closed exposure systems, as common for aquatic toxicity testing. The dissolution rate reflects the rate of transformation of the particles, and is influenced by the intrinsic properties of the particles including amongst others particle shape, chemical composition, surface charge, surface roughness, and surface coating. Dissolution rates are furthermore impacted by the composition of the exposure medium in terms of temperature, pH, ionic strength, redox conditions, presence of (in)organic ligands, and concentration of dissolved organic matter (DOM).[15] It is theoretically accepted that decreased particles size increases particle solubility in the medium,[16] since the smaller particles provide more surface area and thus more atoms at the surface per unit volume.[17] Reported cases on NP dissolution have suggested that first order rate equations in which surface area is considered, are suited to describe the process.[18,19] It is to be noted that due to the combined impact of the various particle and medium properties on the kinetics of dissolution, it is difficult to experimentally demonstrate the effect of one factor in isolation. The starting hypothesis of our research is therefore that dissolution rate constants of metal-bearing NPs depend on the composition and the surface modification of the particles, and this hypothesis is assumed to be suited as a basis for modelling dissolution kinetics based on the pseudo-first order rate constant, with the rate of dissolution of a specific NP at the particle surface being constant and independent of for instance particle size. It is assumed that the mathematical model we aim to develop for quantifying dissolution kinetics allows for categorisation of NPs with a common fate potential, and the model is hypothesized to ultimately assist in screening and grouping of NPs with similar dissolution kinetics, and has high potential of being applicable for newly to be developed NPs.

The aims of our research are:

1) To derive a generic model quantifying the dissolution kinetics of nanoparticles, as applicable to spherical nanoparticles. To address this aim, we developed a mathematical approach which can be used for any exposure medium and in which the dissolution rate constant k can be quantified either as a discrete value or as a range. Consistent with the reduction of the diameter of dissolving particles, the mathematical approach is also applicable to calculate dynamic particle size distributions as a function of exposure time: all that is to be done is to integrate the quantitative dissolution model over the various particle sizes.

2) To compare the model results with experimentally derived data, with the focus on spherical particles. To do so, we collected secondary data on the dissolution profiles of metal-bearing nanoparticles. The data set includes nanoparticles with dissolution kinetics ranging from low (negligible) dissolution rate constants to particles that quickly dissolve with very low half-lives. Literature was screened systematically on nanomaterials dissolution studies published from 2010 to 2020.

2. Methods and materials

Dissolution of metal-bearing NPs refers to the process by which metal ions are released from the surface of the particles when they come into contact with a specific solution. In order to obtain the values of the dissolution rate constants, we have gathered relevant data from previously published papers that specifically address dissolution process (ESI† S1.1). In order to determine the dissolution rate constants, we have developed a mathematical model that enables us to accurately assess the initial part of dissolution process. The process of calculating the dissolution rate constants involves two distinct steps. In the step 1, we carefully extract the relevant data from the published papers and compile them for analysis. The following criteria outline the data required for the model:

1 – Primary physicochemical characteristics of the NPs investigated: elemental composition, diameter, shape, density, and type of coating/doping;

2 – Basic information of the NP suspensions: initial particle concentration and exposure time;

3 – Environmental factors such as medium composition, DOM concentration, pH and ionic strength.

The first step allows to calculate the rate of formation of metal ions on the basis of experimental data at sufficient short exposure times in order to warrant lack of equilibration. The first step can serve as the basis for modelling the kinetics and associated rate constant for dissolution of soluble NPs (ESI† S1.2). After obtaining the ion concentration of the NP from step 1, we can utilize this data to apply it in our dissolution model. The dissolution model for NPs was derived on the basis of the following assumptions:

- A NP is a sphere and it will remain to be a sphere when ions dissolve from it.

• Dissolution is a continuous process in the sense that the radius of the NP decreases continuously when ions dissolve from the NP.

• The dissolution rate constant at the surface of a particle is a constant and this constant is related to the intrinsic properties of an NP in terms of for instance chemical composition and coating, and the extrinsic properties of the medium in terms of for instance DOM concentration, pH and ionic strength.

We formulated a model describing the initial kinetics of the dissolution curve, and the proposed model remains applicable only up to steady state conditions as during the saturation of dissolution process, the ions are released from the particle surface and also reattach back onto the surface.

To model the release of the ions from the spherical particle, we define:

$R(t)$: radius of a NP in cm with $R_0 = R(0)$;

$V(t) = \frac{4}{3}\pi R^3$: volume of a NP;

$A(t) = 4\pi R^2$: area of a NP;

k: dissolution rate constant at the surface of the NP in g cm^{-2} h^{-1};

ρ: density of the particle g L^{-1};

t: time in h;

N_0: number of NPs present in 1 liter of suspension per liter at $t = 0$ in unit of L^{-1}.

$C_{NP}(t)$: concentration of the NPs at time t in g L^{-1};

$C_{ion}(t)$: concentration of the ions at time t in g L^{-1};

The concentrations of NPs and ions at time t are given by:

$$C_{NP}(t) = N_0 \rho V(t), \tag{1}$$

At time $t = 0$, we determine N_0 as,

$$N_0 = \frac{C_{NP}(0)}{\rho V(0)}. \tag{2}$$

First, we present a model for a single NP which has a radius R_0 at $t = 0$.

$$\rho \frac{dV}{dt} = -kA = -k4\pi R^2. \tag{3}$$

The change of ions concentration in the solution becomes:

$$\frac{dC_{ion}}{dt} = N_0 kA = N_0 k4\pi R^2. \tag{4}$$

with $R(0) = R_0$. After particles start to dissolve, the radius of the particle becomes smaller, which means that $R(t)$ in eqn (4) is determined by the duration of dissolution and the initial radius R_0. The density of the particle is not influenced and stays constant through the whole process. Next, by substituting $V(t) = \frac{4}{3}\pi R^3$ into eqn (4) and solving the resulting equation, we obtain the following expression for $R(t)$:

$$R(t) = R_0 - \frac{k}{\rho}t \text{ for } t \le \frac{R_0\rho}{k}, \tag{5}$$

and for $t \ge \frac{R_0\rho}{k}$, $R(t) = 0$.

Also:

$$C_{ion}(t) = \frac{4\rho\pi}{3} N_0 \left[{R_0}^3 - \left(R_0 - \frac{k}{\rho}t \right)^3 \right] + C_{ion}(0) \text{ for } t \le \frac{R_0\rho}{k}, \tag{6}$$

and

$$C_{ion}(t) = \frac{4\rho\pi}{3} {R_0}^3 N_0 + C_{ion}(0) \text{ for } t \ge \frac{\rho R_0}{k}. \tag{7}$$

The concentration of ions and particles present in the suspensions with N_0 particles can be obtained by substituting eqn (1) into eqn (6) and (7):

$$C_{ion}(t) = \left[1 - \left(1 - \frac{kt}{\rho R_0} \right)^3 \right] C_{NP}(0) + C_{ion}(0) \left(\text{for } t \le \frac{R_0\rho}{k} \right), \tag{8}$$

and

$$C_{ion}(t) = C_{NP}(0) + C_{ion}(0) \text{ for } t \ge \frac{\rho R_0}{k} \tag{9}$$

$$C_{NP}(t) = C_{NP}(0) + C_{ion}(0) - C_{ion}(t). \tag{10}$$

The data of $C_{ion}(t)$ and other values were extracted from the curves and manuscripts, and we could transform eqn (8) into:

$$k = \frac{\left(1 - \sqrt[3]{1 - \frac{C_{ion}(t) - C_{ion}(0)}{C_{NP}(0)}} \right) \rho R_0}{t}. \tag{11}$$

The dissolution rate constant k (g cm^{-2} h^{-1}) of NPs, which is the key property for this study, is thus directly calculated by means of eqn (11). The constant is associated with the composition of the particles and the properties of the exposure medium.

In this research, we prepared two sets of methods to determine the dissolution rate constant. Set 1 (ESI† S1.2) is for the generation of as reliable estimates of the initial kinetics of dissolution, including the ion concentration at a certain time point. This set is needed because of the experimental uncertainties and different preparation procedures, lack of duplication of individual measurements, uncertainties in timing of the sampling, *etc.* All these factors will result in discrepancies between cases and set 1 can unify the original data and generate the curves in the formal standard. After obtaining the processed values from the curves, we can use (eqn (11)), which is the actual modelling efforts, to calculate the dissolution rate constant. This quantitative dissolution

model allows to determine the dissolution of metal-bearing nanoparticles, which relate to both particle composition and surface chemistry and exposure medium properties, to provide more accurate data to the latter risk assessment. Please note that the same approach is applicable to any transformation process of spherical particles.

3. Results and discussion

3.1. Literature data search and data mining

From the secondary literature, it was possible to depict dissolution profiles for 4 metal-based NPs including silver (Ag), copper (Cu), copper oxide (CuO) and zinc oxide (ZnO) in 11 kinds of exposure media. This provided 59 estimates of the dissolution rate constant k (Table 1). To further screen for irregular values, the units of all k-values were harmonized (ng cm^{-2} h^{-1}). As shown in Table 1, all values of k fell in a reasonable range varying from 0.004 to 341.7 ng cm^{-2} h^{-1}. The data points for silver nanoparticles constituted almost half of the whole set of dissolution data of NPs. The k values for these Ag NPs ranged from 0.1–472.1 ng cm^{-2} h^{-1} and the mean rate constant was 37.0 ng cm^{-2} h^{-1}. Across the four metal-based nanomaterials, the mean value of k of zinc nanoparticles was the lowest, equaling 0.5 ng cm^{-2} h^{-1}. The highest mean rate constant of nanoparticles was 73.0 ng cm^{-2} h^{-1} for the dissolution of Cu/CuO NPs, indicating that on average Cu/CuO NPs dissolved faster than any of the other NPs in the tested aqueous environments. These wide range of dissolution rates here verified the statement of ref. 20 that composition of the particle was a predominant determinant of dissolution.

For instance, the mechanism of dissolution of most metal-bearing NPs has been reported and follows the same pattern except for Ag NPs. Ion release from Ag NPs is an oxidation process involving protons and dissolved oxygen, which under some conditions proceeds to full reactive dissolution.[21] The reaction can be described as:

$$2Ag(s) + \frac{1}{2}O_{2(aq)} + 2H^{+}_{(aq)} = 2Ag(aq)^{+} + H_2O_{(l)} \qquad (12)$$

Protons and dissolved oxygen play essential roles in Ag NPs surface oxidation and any variation of pH or oxygen saturation of the medium will impact the dissolution kinetics of Ag NPs.

In previous cases, a first-order rate equation has been proposed as an adequate model for describing the dissolution processes of metal-bearing NPs. Several studies have employed the Noyes–Whitney rate equation to model the dissolution of metal and metal oxide NPs,[22,23] and a more general accepted model in the field of geochemistry, which involves normalizing the dissolution rate constant with respect to the surface area by employing a first-order rate equation, as defined by Bruner and Tolloczko.[19] In contrast to these models that solely focus on the saturation concentration and overlook the variations in ion concentration throughout the dissolution process, our model takes into account these changes. We recognize the importance of considering the dynamic nature of ion concentration during the initial stage of dissolution, resulting in a more comprehensive and accurate representation of the process. Furthermore, our model addresses the uncertainty stemming from experimental discrepancies by employing a preprocessing step for the extracted raw data (ESI† S1.1). This preprocessing stage helps mitigate the impact of experimental variations and ensures a more reliable and consistent dataset for analysis. By incorporating this crucial step, our model is better equipped to handle experimental data and provide standardized results for the dissolution process.

When integrated with the two relevant sections, namely the consideration of ion concentration dynamics and the preprocessing of raw data, our model becomes a powerful tool for effectively understanding and predicting the dissolution process. It enables researchers to account for the intricate changes in ion concentration and minimize the influence of experimental uncertainties, thereby improving the overall reliability and applicability of the model in various material science and engineering applications.

3.2. Effects of physico-chemical properties of the NPs on the dissolution rate constant

3.2.1. Size distribution. By definition, smaller particles have a higher specific surface area and more atoms per unit volume at their surface for reaction and this substantially enhances the dissolution process in terms of the overall kinetics of ion release.[34] The rate of release of metal ions is proportional to the specific surface area under specific exposure conditions and nanoparticles are thus expected to dissolve faster than their corresponding macrosized particles according to the Noyes–Whitney equation.[32] The diameter of NPs as collected within the database ranged from 2.4 to 250 nm, with 59 data points available on dissolution kinetics from 12 studies (Fig. 1).

In this research, four types of spherical Cu NPs with diameter 12.5, 25 and 50, were applied in the dissolution test and the value of k was calculated as being 0.04, 0.04 and 0.07 ng cm^{-2} h^{-1}, respectively. These findings thus confirmed our hypothesis of NPs of the same composition having similar rate constants as determined by surface chemistry and medium properties. While there is no doubt about the size as a critical property in the nanomaterial characterization, we explain the absence of a significant correlation between the size of NPs and the dissolution rate constant, as observed in many studies, by considering that the rate constant is primarily influenced by surface and medium properties, and size had a greater impact on the dissolution profile with regard to the time needed to reach steady and the steady state ion concentration. In the case of CuO NPs, the experimental data showed for instance an increase of the final equilibrium concentration upon reduction of particle size (Table 1). The results obtained for Ag NPs reflected that a non-linear, non-monotonic relationship existed between Ag

Table 1 Overview of the experimental dissolution profiles of spherical metal-bearing nanoparticles as retrieved from selected studies

Nominal size (nm)	k (ng cm^{-2} h^{-1})	Time needed to reach steady (h)	Steady state concentration of ions (μg L^{-1})	Initial particle concentration (g L^{-1})	Coating	External variables	Ref.
Silver (Ag) nanoparticles							
4.8	7.6	—	—	5.0×10^{-5}	Citrate	4 °C in DI water	21
4.8	13.8	—	—	5.0×10^{-5}	Citrate	20 °C in DI water	
4.8	24.6	12	41.3	5.0×10^{-5}	Citrate	37 °C in DI water	
4.8	10.2	96	45.9	5.0×10^{-5}	Citrate	DI water	
4.8	7.0	96	25.7	5.0×10^{-5}	Citrate	Seawater buffer	
4.8	3.8	96	17.0	5.0×10^{-5}	Citrate	Natural seawater	
20	23.8	144	93.0	3.0×10^{-4}	Citrate	1/4 Hoagland solution	24
20	5.9	192	150.0	6.0×10^{-4}	Citrate	1/4 Hoagland solution	
40	35.6	48	51.0	3.0×10^{-4}	Citrate	1/4 Hoagland solution	
40	23.6	192	108.0	6.0×10^{-4}	Citrate	1/4 Hoagland solution	
80	25.6	48	30.0	3.0×10^{-4}	Citrate	1/4 Hoagland solution	
80	19.2	72	42.0	6.0×10^{-4}	Citrate	1/4 Hoagland solution	
38	0.02	240	2.7×10^{3}	5.7	PVP	0.001 mol L^{-1} Na_2S in 0.01 M $NaNO_3$	25
38	1.7	60	1.2×10^{4}	1.0	PVP	0.01 M $NaNO_3$	
21	472.1	2	27.5	1.0×10^{-4}	Citrate	DI water	26
21	280.4	4	29.6	1.0×10^{-4}	Citrate	PFCAs with carbon chain length C2	
21	170.5	3	19.4	1.0×10^{-4}	Citrate	PFCAs with carbon chain length C4	
21	129.9	3	12.8	1.0×10^{-4}	Citrate	PFCAs with carbon chain length C7	
115	0.1	24	8.0×10^{4}	1.0	—	Pristine NPs in ALF	27
115	0.1	48	7.3×10^{4}	1.0	—	10 mM CA in ALF	
115	0.1	24	6.6×10^{4}	1.0	—	10 mM TA in ALF	
115	3.3	48	4030.0	1.0	—	Pristine NPs in Gamble solution	
115	3.3	24	3320.0	1.0	—	10 mM CA in Gamble solution	
115	3.6	48	5430.0	1.0	—	10 mM FA in Gamble solution	
115	3.2	24	3700.0	1.0	—	10 mM TA in Gamble solution	
115	2.2	48	2080.0	1.0	—	Pristine NPs in modified ALF	
115	2.5	48	2250.0	1.0	—	10 mM CA in modified ALF	
115	1.5	48	1290.0	1.0	—	10 mM FA in modified ALF	
115	2.9	48	2330.0	1.0	—	10 mM TA in modified ALF	
115	2.1	12	1160.0	1.0	—	Pristine NPs in Gamble solution	
115	2.2	12	1230.0	1.0	—	10 mM CA in modified Gamble solution	
115	1.6	12	882.0	1.0	—	10 mM TA in modified Gamble solution	
15	8.5	48	119.7	1.0×10^{-3}	—	Tested soil extract	28
30	1.8	48	94.2	1.0×10^{-3}	—	Tested soil extract	
Copper/copper oxide (Cu/CuO) nanoparticles							
25	0.04	24	114.4	0.2	—	Cell culture media	[8]
50	0.04	24	72.9	0.2	—	Cell culture media	
250	0.5	24	107.7	0.2	—	Cell culture media	
25	11.6	24	2.9	1.0×10^{-5}	—	Standard test medium	29
50	14.9	24	2.1	1.0×10^{-5}	—	Standard test medium	
100	56.8	24	2.5	1.0×10^{-5}	—	Standard test medium	
250	341.7	216	2.2	1.0×10^{-5}	—	Standard test medium	
40	66.6	34	550	1.0×10^{-3}	—	DI water	30
40	32.4	40	390	1.0×10^{-3}	—	Groundwater	
40	74.4	—	—	1.0×10^{-3}	—	Natural water	
25	4.85	48	287.3	1.0×10^{-3}	—	Tested soil extract	31
50	3.12	24	172.0	1.0×10^{-3}	—	Tested soil extract	
100	8.60	72	222.7	1.0×10^{-3}	—	Tested soil extract	
500	71.63	24	368.7	1.0×10^{-3}	—	Tested soil extract	
Zinc oxide (ZnO) nanoparticle							
2	0.004	0.5	1310.0	1.0	—	pH 11 of medium	32
2	0.1	0.5	5670.0	1.0	—	pH 9 of medium	
2	0.3	1	8830.0	1.0	—	pH 6 of medium	
2	0.7	1	3.0×10^{4}	1.0		pH 3 of medium	
2	0.1	1	7.2×10^{4}	1.0		pH 1 of medium	
20	0.1	72	850.0	0.7	—	2 mM K_2HPO_4 in 10 mM $NaNO_3$ solution	33
20	0.04	120	220.0	0.7	—	5 mM K_2HPO_4 in 10 mM $NaNO_3$ solution	
18	1.76	—	368.8	1.0×10^{-3}	—	Tested soil extract	31
43	1.84	—	356.1	1.0×10^{-3}	—	Tested soil extract	

DI water: deionized water; PFCAs: perfluorocarboxylic acids; C2/C4/C7: carbon chain length; CA: citric acid; FA: fulvic acid; TA: tartaric acid; ALF: artificial lysosomal fluid.

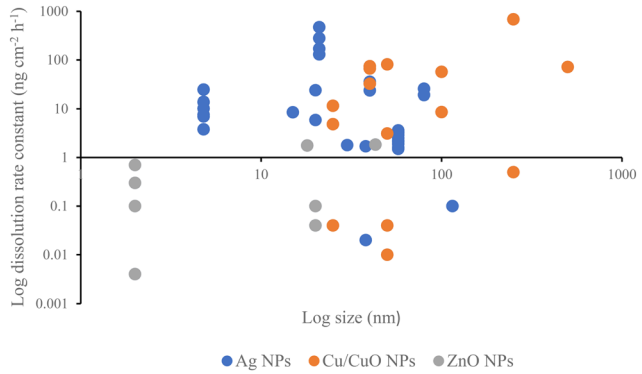

Fig. 1 The relationship between NPs sizes and dissolution rate constants. Log-transformed dissolution of rate constants of NPs are plotted on the *y*-axis and log-transformed sizes are plotted on the *x*-axis.

dissolution and size, which can be attributed to the surface modification observed on Ag NPs and had a significant impact on the solubility of the NPs.[1] More details on surface modifications can be found in section 3.2.2.

According to a previous report on dissolution rates, the size effect of primary NPs on dissolution can only be observed when the particles sizes fall in a certain range, lower than 20 nm.[35] Theoretically, rate constants generated from the model should be similar across different size range as long under the same treatment, and our modelling results did not provide evidence on the presence of a statistically significant correlation between the calculated values of k and the reported particle size across the NPs studied (Fig. 1 and Table 2).

3.2.2. Surface modification and dissolution rates. The surface chemistry dependent solubility has been studied extensively for Ag NPs, and it was shown that capping agents can considerably influence the rate of dissolution of Ag NPs (Table 1). It was found that the mean value of k of coated Ag NPs was 69.7 ng cm^{-2} h^{-1} and the mean value of k of uncoated Ag NPs was 2.4 ng cm^{-2} h^{-1}. For the other metal-based NPs we could not find both coated and uncoated dissolution rate constant data; therefore, no comparison could be made.

Polyvinylpyrrolidone (PVP) and citrate capped Ag NPs have commonly been used for toxicity studies and based on available data, it is evident that various capping agents have distinct effects on the dissolution of Ag NPs. For example, 50 nm Ag NPs PVP capped particles showed 50% dissolution at 25 °C in water after 125 days of exposure, compared to 14% dissolution for citrate capped Ag NPs of the same size exposed at the same exposure conditions and exposure duration.[37] On the contrary, it's[38] observed that citrate capped Ag NPs (71 nm) had a higher dissolution rate compared to PVP-Ag NPs (67 nm) in water over a 30 min exposure period. Based on our foundings, it can be concluded that the coating composition is an crucial particle property affecting dissolution. However, it's difficult to identify a specific trend regarding the impact of coating on dissolution. Among the coating agents commonly applied, citrate coating was the most frequently mentioned in three papers (18 data points) and four research reports also confirmed that coated Ag NPs were less stable and released more ions than non-coated Ag NPs.[21,24–26]

Most of the commercial NPs have core–shell structures with organic coatings, and coatings which serve as both the initial reducing agent and stabilizer.[26] The results of Angel[39] showed that citrate stabilized silver particles exhibit a higher dissolution rate in an aquatic medium than PVP surface-stabilized Ag NPs. On the other hand, citric coating may also enhance ion release from the particles, and the release of dissolved Zn ions from citric coated ZnO NPs was approximately 10% higher than Zn ion release from pristine ZnO NPs.[27] Ortelli[40] reported on the other hand that different organic coating agents did not affect the CuO NPs stability in artificial marine water due to the high ionic strength of the medium. Meanwhile, these coatings could also change the reactive surface area by inducing aggregation of the particles.[14] The results shown in our study indicate that relying solely on one metric may not be a reliable approach for understanding and predicting the dissolution of NPs. The combination of different properties must be included and these combinations are more relevant as a group than a single metric alone.

Table 2 Impact of nanoparticle radius on dissolution rate constants

NPs	Radius (nm)	k (ng cm^{-2} h^{-1})	Ref.
Ag	2.4	3.8–24.6	21
Ag	10–40	5.9–35.6	24
Ag	19.5	0.02–1.7	25
Ag	25	0.1–3.6	27
Ag	15–30	1.75–8.5	28
Cu	12.5–250	0.04–0.5	8
Cu	12.5–250	11.6–341.7	29
Cu	25	81	36
Cu	25–250	3.1–71.6	31
CuO	20	32.4–74.4	30
ZnO	2	0.04–0.7	32
ZnO	20	0.04–0.1	33
ZnO	18–43	1.7–1.8	31

k = dissolution rate constant (ng cm^{-2} h^{-1}).

3.3. Impact of the exposure medium (composition, pH, ionic strength (IS) and dissolved organic matter (DOM)) on dissolution rates

Upon thorough analysis of all existing studies, we have successfully incorporated the assessment of exposure conditions into our evaluation, taking into account their potential impact on the dissolution of NPs. The collected database showed that three main categories of media were investigated: deionized water (n = 12), natural water including river, lake and seawater (n = 2) and media mixed with organic or inorganic matter (n = 45).

The water chemistry of the exposure medium in terms of pH, IS and DOM, was found to have an important impact on the particle dissolution process.[36] The stability of metal oxide nanoparticles in aqueous suspensions depends to a large extent on the IS.[32] As the IS increases, the ζ-potential is reduced and the nanoparticle surface charge is modified due to adsorption of counterions. This will promote agglomeration and suppress dissolution.[30] The dissolution rates have been demonstrated to be affected by pH levels, for instance: at pH 1.0, 92% ion release from ZnO NPs was observed and only around 15% of the total mass of ZnO NPs dissolved when pH was 6.[32] This finding may amongst others be due to the low dissolved humic acid concentration and protonation of carboxylic and phenolic groups on humic acid at low pH, which reduced the activity and accessibility of these functional groups to adsorb to the ZnO NPs. Dissolved organic matter in natural waters is also known as an agent in improving the stability of nanoparticles. In general, increased dissolution rates of metal-bearing NPs have been reported in the presence of DOM and this effect is the same as expected for larger sized particles. Focusing on the rate constant k, it can be observed from Table 3 that it ranged from 3.8–24.6 ng cm^{-2} h^{-1} for 4.8 nm silver NPs[21] when the concentration of DOM in the medium was increased in between 0–50 mg L^{-1}. As an increased dissolution is connected to a relatively high affinity of the functional groups of DOM to the particles surface, especially in medium at high pH (pH 9–11) where the hydroxide layer formed on the surface of NPs could inhibit further dissolution under alkaline conditions[32] and similar results from Vencalek[30] also showed that the composition of the exposure medium had a huge impact on the rate constant. This phenomenon has been observed only in the case of ZnO, and it would be inappropriate to apply this mechanism to other types of nanomaterials without sufficient supporting evidence. It is noted that the mean values of k in natural water (river water with 1 mg L^{-1} DOM[30]) was 74.4 ng cm^{-2} h^{-1}, which is higher than the mean rate constant in deionized water and groundwater without DOM (49.5 ng cm^{-2} h^{-1}) in the same experimental set up, and thus confirming that the constant could also be independent to the DOM. Likewise, DOM could be used as "thick coating layer" to inhibit the light absorption by NP surfaces and prevent the interactions between dissolved oxygen and particles, which further weakens the dissolution of Ag NPs.[26,41]

HA, which accounts for a large portion of the DOM in natural aquatic environment, appeared in 5 papers included in the database. It has been reported that ionic Ag concentration increased with increasing HA concentration in the first 24 h of exposure when the HA concentration ranged from 0–20 mg L^{-1}.[42] On the other hand, longer term (150 d) tracking showed that the dissolution of Ag NPs decreased with time after prolonged periods of exposure at the same HA concentration. An increased dissolution by the addition of tannic acid (TA) was also observed. For instance: in a 20 mM $NaNO_3$ electrolyte solution, dissolution of CuO NPs increased with increasing TA concentrations of at least 14.7 μM.[43] However, former study reported that the presence of cations in the medium could reduce the dissolution of CuO NPs by HA and the underlying mechanism could be: (a) ions in the medium compete with HA functional groups for Cu ions released from NP surface, occupying some HA and hindering complexation of additional Cu ions which reduces driving force for dissolution; (b) cations occupy HA functional groups and decrease HA–NP interaction.[44] Other environmental factors also exert an impact on the dissolution rate of specific NPs. For instance, the oxidative dissolution of Ag NPs is modulated by the dissolved oxygen concentration and light intensity.[26]

In summary: the properties of the exposure medium, such as ionic strength (IS), pH, and dissolved organic matter (DOM), play a crucial role in determining the dissolution rate

Table 3 Effect of three main types of medium (DI water/ media mixed with organic or inorganic matter/ natural water) properties on dissolution rate constants

Medium	Composition	pH	k (ng cm^{-2} h^{-1})	DOM (mg L^{-1})	Ref.
DI water	Ag	5.6	3.8–24.6	0–50	21
DI water	ZnO	6	0.04–0.7	0–100	32
DI water	CuO	7.7 ± 0.3	66.6	—	30
100 mL modified quarter-strength Hoagland medium	Ag	5.6	5.9–35.6	—	24
0.01 M $NaNO_3$ solution	Ag	7.0 ± 0.2	0.02–1.7	—	25
$CaCl_2{\cdot}2H_2O$: 294; $MgSO_4{\cdot}7H_2O$: 123.25; $NaHCO_3$: 64.75; KCl: 5.75 (mg L^{-1}, MilliQ water)	Cu	7.8 ± 0.2	11.6–341.7	—	29
Artificial lysosomal fluid (ALF)	Ag	4.5	0.1–3.6	0–300	27
$CaCl_2{\cdot}2H_2O$: 294; $MgSO_4{\cdot}7H_2O$: 123.25; $NaHCO_3$: 64.75; KCl: 5.75 (mg L^{-1}, MilliQ water)	Cu	4	0.04–0.5	—	8
$CaCl_2{\cdot}2H_2O$:294; $MgSO_4{\cdot}7H_2O$: 123.25; $NaHCO_3$: 64.75; KCl: 5.75 (mg L^{-1}, MilliQ water)	CuO	7.8 ± 0.2	81	1	36
10 mM Bis–Tris buffer	Cu	7	3.1–71.6	—	31
0.01 M $NaNO_3$ solution	ZnO	7.0 ± 0.2	0.04–0.1	—	33
Groundwater	CuO	7.7 ± 0.3	32.4	—	30
Natural water	CuO	6.7–9.1	74.4	1	30

DI water: deionized water.

of nanoparticles in aqueous suspensions. Changes in IS alter the ζ-potential and surface charge of nanoparticles, potentially leading to agglomeration and suppression of dissolution. Meanwhile, a decrease in pH has been observed to lead to increased dissolution. The presence of DOM can also impact the stability of nanoparticles, with increasing DOM concentration resulting in a higher dissolution rate constant. Studies have shown that the presence of humic acid (HA), can both increase and decrease the dissolution of metal-bearing NPs over time, depending on the HA concentration and presence of cations in the medium. Other environmental factors, such as dissolved oxygen concentration and light intensity, can also affect the dissolution rate of specific nanoparticles. The analysis of particle and ion complexation can help to predict the environmental behavior and toxicity of NP suspensions.

In the static (quasi-equilibrium) system commonly used for toxicity testing, the ions that are liberated from the NPs *via* dissolution are finally dissolved in the suspension media. Dissolution may continue for a considerable time, but eventually the ion concentration stabilizes and remains constant, to reach a steady state ion concentration. Meanwhile, the kinetics of dissolution and the saturation concentration may vary for the same NPs when suspended in different exposure (environmental, biological) media. It is therefore highly relevant to discuss equilibration times and the resulting steady state levels. For the metal-bearing NPs discussed above, the time needed to reach steady state levels of dissolution relied on both external and internal properties. In batch studies, as performed in the studies selected, the dissolution process is slowed down because of the driving force for dissolution being reduced upon increasing ion concentrations. This finally leads to a pseudo-equilibrium as at a certain moment, there is no driving force left for ions to go into suspension. This setting is for instance typical for toxicity testing conditions in which a relatively large number of NPs are suspended in a relatively low volume of exposure medium.

The time needed to reach steady state of the ions concentration ranged from 0.5 to 240 hours (Table 1), depending on both particles and medium properties in the different cases present in the database. The size and initial concentration of the NPs in the suspensions also had an impact on the time needed to reach equilibrium. Higher numbers of larger particles in the suspensions increase the likelihood of particle–particle interactions, thereby reducing the dissolution rate. However, insufficient exposure duration can lead to the "absence" of equilibrium, wherein the ion concentration continues to increase during the whole measurement.[21,30] or the suspensions gets saturated before the first measured time point.[31] In the case of Zhang,[24] it took 48 hours for 80 nm Ag NPs to reach equilibrium at the ions concentration of 30 $\mu g\ L^{-1}$ while only after 192 hours of exposure, the ion concentration in a suspension of 20 nm Ag NPs stabilized at a concentration of 150 $\mu g\ L^{-1}$ in the same medium. The dissolution process is slowed down for the smaller sized NPs, which could be accounted for by the total amount of released Ag ions from the 20 nm Ag NPs being higher than in case of the 80 nm Ag NPs, with dissolution being reduced upon increasing ion concentrations. The dissolution rate constant will to some extent depend on how far from equilibrium the system is with respect to precipitation and metal ion complexation with ligands such as DOM. Thus, the time needed to reach equilibrium and steady state of the ion concentration reflects how particles properties and environmental factors impact dissolution.

3.4. The application of the model in future regulation

Our modelling approach provides a starting point from which to integrate the data of dissolution curves of metal-bearing NPs in different media as reported in the period 2010–2020 for the development of a generic model to determine dissolution rate constants and predict the whole time-course of dissolution. The results confirmed that the composition of both the NPs and the exposure medium had a huge impact on the rate constants.

Further application in assessing the toxicokinetics of metal-bearing NPs could be validated based on the work in this research. Our model reduces the work of the ecotoxicity experiments and will be a powerful tool in the assessment and prediction of nanosafety issues. It is noted that animal/plant experiments are irreplaceable because they could provide data and information to support nanotoxicological studies. Meanwhile, one research gap is needed to be identified: the kinetics of dissolution and the overall ion release profile need to be experimentally determined during toxicity testing as it is not yet possible to model or predict the overall dissolution curves for specific nanomaterials. Overall, as with any model, the data quality influences the performance of our model.

Given the limited number of publications available in the database, the calculated rate constants from the model should be treated with caution. In the present work, the factors determining dissolution rate constants of NPs were successfully screened by integrating data mined from the literature. To build a better connection between the model and dissolution of NPs, the impact of particle surface modification and medium water chemistry on the rate constant could be quantified in the next generation of dissolution models. This requires more data from realistic experimental exposure scenarios. But still, our model could act as the best model to determine the ion release kinetics and it could be extended to act as the first screening step of newly upcoming NPs, distinguishing their toxicity based on their dissolution rate constant under different scenarios, which could contribute to the knowledge in the environmental risk assessment of metal-bearing NPs.

4. Conclusions

Innovations in nanotechnology and in the incorporation of nanoparticles in a wide range of products, cause the release of NPs into the environment. Within all the dynamic

transformations that NPs go through, dissolution assessment has the potential to become a key component of a fast screening process for categorising NPs with a common fate potential. According to the data collected in this study, a first order rate equation is suited to properly describe the initial kinetics of dissolution of NPs in different media and the rate constant can represent the extent of ion release in realistic environmental exposure scenarios. The dissolution rate is dependent on the physico-chemical characteristics of NPs (like composition, morphology, and surface chemistry) and on environmental conditions (especially pH, ionic strength, oxic/anoxic conditions, and natural organic matter). The rate of ion release is dependent on surface area, thus size or diameter of the NP. It is, therefore, possible to calculate the particle dissolution with our pseudo-first order rate constant model. When data on the specific surface of a new NP is available, future grouping approaches on the basis of the dissolution profiles of NPs might be useful for the screening of especially persistent and quickly dissolving NPs. This will significantly speed up the pace of future screening risk assessment of NPs and will in the end allow for prediction of the dissolution kinetics of newly developed nanomaterials.

Conflicts of interest

There are no conflicts to declare.

Acknowledgements

This work was supported by the GRACIOUS project that is part of the European Union's Horizon 2020 research and innovation programme [grant number 760840]. The Chinese Scholarship Council (CSC) is gratefully acknowledged for its financial support to Yuchao Song (201906320061).

References

1 Y. Bi, A. K. Marcus, H. Robert, R. Krajmalnik-Brown, B. E. Rittmann, P. Westerhoff, M. H. Ropers and M. Mercier-Bonin, *J. Toxicol. Environ. Health, Part B*, 2020, **23**, 69–89.
2 O. Bondarenko, K. Juganson, A. Ivask, K. Kasemets, M. Mortimer and A. Kahru, *Arch. Toxicol.*, 2013, **87**, 1181–1200.
3 L. Vittori Antisari, S. Carbone, A. Gatti, G. Vianello and P. Nannipieri, *Soil Biol. Biochem.*, 2013, **60**, 87–94.
4 F. Abdolahpur Monikh, D. Arenas-Lago, P. Porcal, R. Grillo, P. Zhang, Z. Guo, M. G. Vijver and W. J. G. M. Peijnenburg, *Nanotoxicology*, 2020, **14**, 310–325.
5 A. Noori, J. C. White and L. A. Newman, *J. Nanopart. Res.*, 2017, **19**, 1–13.
6 J. Wu, Y. Zhai, F. A. Monikh, D. Arenas-Lago, R. Grillo, M. G. Vijver and W. J. G. M. Peijnenburg, *J. Agric. Food Chem.*, 2021, **69**, 12527–12540.
7 M. F. Hornos Carneiro and F. Barbosa, *J. Toxicol. Environ. Health, Part B*, 2016, **19**, 129–148.
8 L. Song, M. Connolly, M. L. Fernández-Cruz, M. G. Vijver, M. Fernández, E. Conde, G. R. De Snoo, W. J. G. M. Peijnenburg and J. M. Navas, *Nanotoxicology*, 2014, **8**, 383–393.
9 B. Fubini, M. Ghiazza and I. Fenoglio, *Nanotoxicology*, 2010, **4**, 347–363.
10 R. J. Griffitt, K. Hyndman, N. D. Denslow and D. S. Barber, *Toxicol. Sci.*, 2009, **107**, 404–415.
11 K. Luyts, D. Napierska, B. Nemery and P. H. M. Hoet, *Environ. Sci.: Processes Impacts*, 2013, **15**, 23–38.
12 G. Oberdörster, V. Stone and K. Donaldson, *Nanotoxicology*, 2007, **1**, 2–25.
13 A. A. Keller, H. Wang, D. Zhou, H. S. Lenihan, G. Cherr, B. J. Cardinale, R. Miller and Z. Ji, *Environ. Sci. Technol.*, 2010, **44**, 1962–1967.
14 S. K. Misra, A. Dybowska, D. Berhanu, S. N. Luoma and E. Valsami-Jones, *Sci. Total Environ.*, 2012, **438**, 225–232.
15 M. Amde, J. F. Liu, Z. Q. Tan and D. Bekana, *Environ. Pollut.*, 2017, **230**, 250–267.
16 P. Borm, F. C. Klaessig, T. D. Landry, B. Moudgil, J. Pauluhn, K. Thomas, R. Trottier and S. Wood, *Toxicol. Sci.*, 2006, **90**, 23–32.
17 Q. Abbas, B. Yousaf, M. U. Ali, M. A. M. Munir, A. El-Naggar, J. Rinklebe and M. Naushad, *Environ. Int.*, 2020, **138**, 105646.
18 A. A. Noyes and W. R. Whitney, *J. Am. Chem. Soc.*, 1897, **19**, 930–934.
19 L. Bruner and St. Tolloczko, *Z. Anorg. Chem.*, 1901, **28**(1), 314–330.
20 L. M. Stabryla, K. A. Johnston, J. E. Millstone and L. M. Gilbertson, *Environ. Sci.: Nano*, 2018, **5**, 2047–2068.
21 J. Liu, D. A. Sonshine, S. Shervani and R. H. Hurt, *ACS Nano*, 2010, **4**, 6903–6913.
22 T. S. Peretyazhko, Q. Zhang and V. L. Colvin, *Environ. Sci. Technol.*, 2014, **48**, 11954–11961.
23 S. M. Majedi, B. C. Kelly and H. K. Lee, *Sci. Total Environ.*, 2014, **496**, 585–593.
24 W. Zhang, Y. Yao, N. Sullivan and Y. Chen, *Environ. Sci. Technol.*, 2011, **45**, 4422–4428.
25 C. Levard, B. C. Reinsch, F. M. Michel, C. Oumahi, G. V. Lowry and G. E. Brown, *Environ. Sci. Technol.*, 2011, **45**, 5260–5266.
26 Y. Li, J. Niu, E. Shang and J. Crittenden, *Environ. Sci. Technol.*, 2014, **48**, 4946–4953.
27 L. Zhong, X. Hu, Z. Cao, H. Wang, Y. Chen and H. Lian, *Chemosphere*, 2019, **225**, 668–677.
28 Y. Zhai, E. R. Hunting, M. Wouters, W. J. G. M. Peijnenburg and M. G. Vijver, *Front. Microbiol.*, 2016, **7**, 1–9.
29 L. Song, M. G. Vijver, G. R. de Snoo and W. J. G. M. Peijnenburg, *Environ. Toxicol. Chem.*, 2015, **34**, 1863–1869.
30 B. E. Vencalek, S. N. Laughton, E. Spielman-Sun, S. M. Rodrigues, J. M. Unrine, G. V. Lowry and K. B. Gregory, *Environ. Sci. Technol. Lett.*, 2016, **3**, 375–380.
31 Y. Zhai, E. R. Hunting, M. Wouterse, W. J. G. M. Peijnenburg and M. G. Vijver, *Ecotoxicol. Environ. Saf.*, 2017, **145**, 349–358.
32 S. W. Bian, I. A. Mudunkotuwa, T. Rupasinghe and V. H. Grassian, *Langmuir*, 2011, **27**, 6059–6068.
33 J. Lv, S. Zhang, L. Luo, W. Han, J. Zhang, K. Yang and P. Christie, *Environ. Sci. Technol.*, 2012, **46**, 7215–7221.

34 T. Diedrich, A. Dybowska, J. Schott, E. Valsami-Jones and E. H. Oelkers, *Environ. Sci. Technol.*, 2012, **46**, 4909–4915.
35 M. D. Scanlon, P. Peljo, M. A. Méndez, E. Smirnov and H. H. Girault, *Chem. Sci.*, 2015, **6**, 2705–2720.
36 Y. Xiao, K. T. Ho, R. M. Burgess and M. Cashman, *Environ. Sci. Technol.*, 2017, **51**, 1357–1363.
37 S. Kittler, C. Greulich, J. Diendorf, M. Köller and M. Epple, *Chem. Mater.*, 2010, **22**, 4548–4554.
38 K. A. Huynh and K. L. Chen, *Environ. Sci. Technol.*, 2011, **45**, 5564–5571.
39 B. M. Angel, *Chemosphere*, 2013, **93**(2), 359–365.
40 S. Ortelli, A. L. Costa, M. Blosi, A. Brunelli, E. Badetti, A. Bonetto, D. Hristozov and A. Marcomini, *Environ. Sci.: Nano*, 2017, **4**, 1264–1272.
41 E. Shi, Z. Xu, X. Zhang, X. Yang, Q. Liu, H. Zhang, A. Wimmer and L. Li, *Environ. Pollut.*, 2018, **243**, 1242–1251.
42 I. Fernando and Y. Zhou, *J. Mol. Liq.*, 2019, **284**, 291–299.
43 J. Zhao, Y. Liu, B. Pan, G. Gao, Y. Liu, S. Liu, N. Liang, D. Zhou, M. G. Vijver and W. J. G. M. Peijnenburg, *Water Res.*, 2017, **127**, 59–67.
44 G. Giovannini, P. Warncke, D. Fischer, O. Stranik, A. J. Hall and V. Gubala, *Nanotoxicology*, 2018, **12**, 407–422.